

Concept Study for the Beamforming Elevated Array for Cosmic Neutrinos (BEACON)

Stephanie Wissel*

California Polytechnic State University, San Luis Obispo, CA USA

E-mail: swissel@calpoly.edu

J. Alvarez-Muñiz¹, C. Burch^{7,10}, W. Carvalho Jr.^{1,2}, A. Cummings³, C. Deaconu⁴, G. Hallinan⁵, K. Hughes⁴, A. Ludwig⁴, E. Oberla⁴, C. Paciaroni⁶, A. Rodriguez⁶, A. Romero-Wolf^{5,7}, H. Schoorlemmer⁹, D. Southall⁴, B. Strutt⁸, M. Vasquez⁶, A. Vieregg⁴, and E. Zas¹

¹*Universidade de Santiago de Compostela*, ²*Universidade de São Paulo*, ³*Gran Sasso Science Institute*, ⁴*University of Chicago*, ⁵*California Institute of Technology*, ⁶*California Polytechnic State University*, ⁷*Jet Propulsion Laboratory*, ⁸*University of California, Los Angeles*, ⁹*Max-Planck-Institut für Kernphysik* ¹⁰*Harvard University*

Tau neutrinos are expected to comprise one third of both the astrophysical and cosmogenic neutrino flux, but currently the flavor ratio is poorly constrained and the expected flux at energies >100 PeV is low. We present a new concept for a radio detector called BEACON sensitive to tau neutrinos with energies greater than 100 PeV in which a radio interferometer searches for upgoing tau neutrinos from a high elevation mountain. Signals from several antennas are coherently summed at the trigger level, permitting not only directional masking of anthropogenic backgrounds, but also a lower trigger threshold. Simulation studies indicate that a modest array size and small number of stations can achieve competitive sensitivity, provided the receivers are at high enough elevation. As a proof of concept, an array of four 30-80 MHz dual polarized antennas was deployed at the White Mountain Research Station.

Acknowledgements We gratefully acknowledge funding from the NSF CAREER Award #1752922, the NSF Award #DGE-1746045, the Cal Poly Frost Fund, the Ministerio de Economía, Industria y Competitividad (FPA2017-85114-P and María de Maeztu Unit of Excellence MDM-2016-0692) and the Xunta de Galicia (ED431C 2017/07) as well as the outstanding staff at WMRS and OVRO and computing resources provided by the Univ. of Chicago Research Computing Center.

*36th International Cosmic Ray Conference -ICRC2019-
July 24th - August 1st, 2019
Madison, WI, U.S.A.*

*Speaker.

1. Motivation

Measuring the neutrino flux above 100 PeV is critical to uncovering the origin of the diffuse fluxes of both the highest energy cosmic rays and the highest energy neutrinos, and neutrino production mechanisms at the sources [1]. Muon and electron neutrinos are expected to be produced through pp and $p\gamma$ interactions by astrophysical accelerators, while tau neutrinos can only arise from oscillations over astrophysical baselines. The tau neutrino flux can not only confirm that the neutrino flux is indeed astrophysical, but also the standard oscillation scenario in a new energy regime [2].

The astrophysical diffuse flux of neutrinos observed by IceCube may extend to higher energies. The spectral index measured with the muon neutrino tracks suggests a hard spectrum of $E^{2.13 \pm 0.13}$ [3], while the spectral indices measured with the cascade events are softer [4, 5]. The diffuse neutrino landscape could very well be a complex combination of multiple unresolved sources that can be better understood by extending the spectrum to higher energies. At 100 PeV, the expected flux from cosmogenic models and extensions to the IceCube flux overlap, making this energy scale a compelling energy range.

To expand the reach of neutrino experiments into the 100 PeV to EeV energy regime requires an improvement in exposure at reasonable cost. We focus here on a concept that aims to maximize single station exposure to upgoing tau neutrinos using a phased interferometer on a high-elevation mountain. Such a concept is scalable in that multiple sites around the world can be used to achieve full sky coverage, which is particularly important for multi-messenger observations.

2. Concept

Several existing and proposed experiments search for the radio emission from upgoing tau lepton decays resulting from tau neutrino interactions in the Earth. The BEACON concept differs in placing a phased interferometer on a high-elevation mountain, as shown in Fig. 1. Mountain ridges of high prominence (> 2 km), the difference between the elevation of the peaks and the viewable valley, maximize the individual station acceptance, while still being close enough to the air showers to maintain a low energy threshold. By phasing multiple antennas together in an interferometer, sub-degree scale pointing can be achieved and background events can be localized and excluded from the trigger.

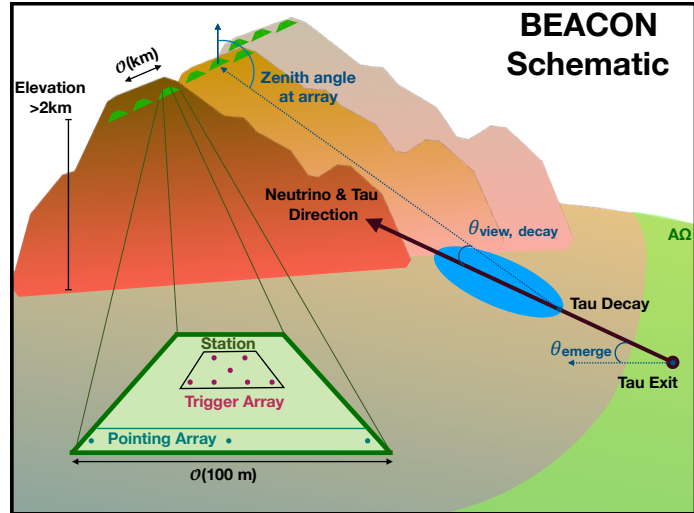


Figure 1: Design concept of BEACON stations.

A dedicated Monte Carlo was developed to simulate the geometric acceptance [6] of a high-elevation detector, the probability that a tau will exit the Earth [7] and decay to produce an air shower, and the probability that the tau will be detected via its radio emission by an interferometer. The results of the simulation (presented in Sections 3, 4, and 5) lead us to a reference design for BEACON that includes 100 stations not necessarily all at the same site. Each station phases together 10 antennas in a low frequency band (30-80 MHz) with a view of 120° , as shown in Fig. 1. Seven antennas are closely packed in a trigger array, while three antennas are further from the center and used for pointing reconstruction in addition to triggering. While the reference design shows assumes a 3 km prominence, our results indicate that only a 2 km elevation is necessary to exploit the geometry.

An important advantage of the high-elevation radio detector design is that the detectors can be placed at multiple sites throughout the world, specifically on any mountain ridge that overlooks a reasonably radio-quiet valley. A global network of high-elevation mountain receivers could achieve full sky coverage, an important requirement for studies of explosive transients [1].

2.1 Radio Detection of Upgoing Tau Air Showers

Upgoing tau neutrinos may be detected via the air showers that result from tau propagation and regeneration through the Earth. Tau neutrinos are expected to interact in the Earth via charged current interactions that produce a tau lepton. The tau lepton decay invariably results in another tau neutrino and this process can repeat until the particles reach the other side of the Earth. When this process results in a τ lepton exiting the Earth, the τ can decay in the atmosphere within a decay length of $L_{decay} = 49 \text{ km} (E_\tau/\text{EeV})$ to produce an air shower. The probability that a tau will exit the Earth depends on energy and emergence angle and is maximized for Earth-skimming configurations with emergence angles $< 3^\circ$ at energies greater than 0.1 EeV [7]. Tau leptons can decay through hadronic channels that produce pions or leptonic channels that produce muons or electrons, but only the hadronic and electronic decays produce air showers. We sample the energy deposition into showers using Pythia [8] simulated tau lepton decays. The energy fraction distribution has an average of 0.56 with a 68% confidence interval of ranging from 0.25 to 0.87.

Radio techniques are a promising method for the detection of ultra-high-energy particle air showers. The primary advantages are the low cost per channel of the instrumentation and the ability to trigger on showers from hundreds of kilometers away. Both are particularly important when considering the low expected flux of tau neutrinos at energies higher than 100 PeV and the geometric considerations associated with triggering on Earth-skimming showers. Air showers produce broadband, impulsive signals at radio frequencies due to a combination of the geomagnetic and Askaryan effects. Radio-based triggers are challenged by the requirement that an experiment trigger on impulsive air shower signals in the presence of man-made radio frequency interference (RFI). Recently cosmic ray experiments have successfully clustered RFI sources [9] and been able to discriminate against them in real time while retaining sensitivity to air shower pulses [10]. Current studies are exploring the use of real-time radio-only triggers in context of a high-elevation mountain [11].

Upgoing tau air showers are expected to generate broadband electric field signals such as those shown in Fig. 2. Using the ZHAireS code [12] for simulation of radio emission from air showers, modified for the treatment of upward-going shower, we simulated showers measured at different

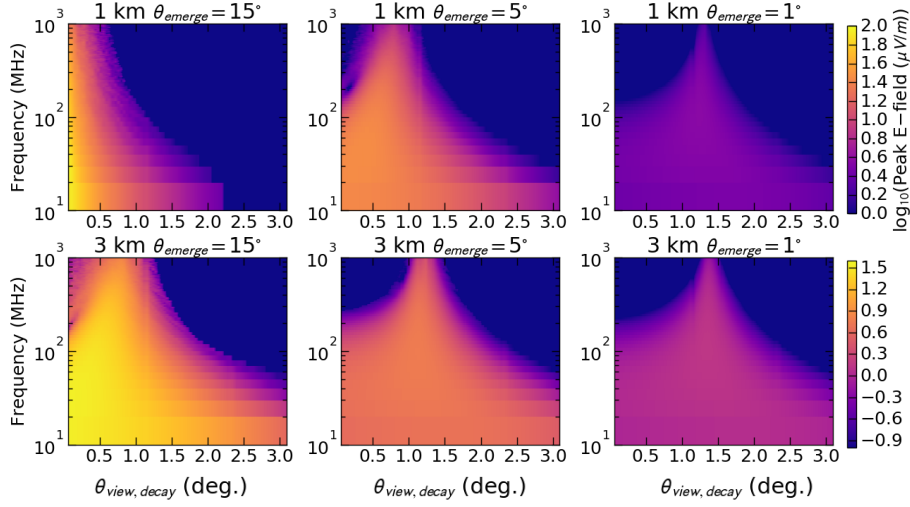


Figure 2: Peak electric field binned in 10 MHz sub-bands from ZHAireS [12] simulations of up-going tau lepton air showers emerging from the earth at an angle of 15° (left), 5°, and 1° above the horizontal. The electric field is measured on detectors that view the shower at angles measured from tau decay point and that are placed at 1 km (top) and 3 km (bottom) elevations.

elevations above sea level as measured by a line of antennas. The complete set of simulations included a range of tau emergence angles from 1° to 35°, view angles $\theta_{view, decay}$ relative to the decay point of the shower (0-3.2°), and tau lepton decay altitudes. ZHAireS simulates the electric field in the time domain. The magnitudes of the peak electric field, E_{peak} are binned in 10 MHz subbands to form the lookup tables shown in Fig. 2. The radio beam is broad at lower frequencies and forms a Cherenkov cone at higher frequencies. The Cherenkov cone notably does not form when the shower is too close to the detector at, for instance, high emergence angles and low detector altitudes.

2.2 Time Domain Interferometry

Digital interferometric triggering in the time-domain has been shown to lower the voltage field threshold of an in-ice radio neutrino experiment [13] and to self-trigger on cosmic ray air showers using hundreds of antennas [10]. When used in the context of BEACON, we can take advantage of several features of phased array triggering to reduce anthropogenic backgrounds at the trigger level and lower the voltage and therefore energy threshold of the detector.

Beams in a particular direction can be formed knowing the precise geometry of the array by delaying and summing waveforms from multiple antennas in the time domain. Digital phased arrays form beams on an FPGA via coherent sums of N antennas at programmable angles. The signal-to-noise ratio (SNR) of a neutrino radio pulse grows as a factor of \sqrt{N} , because the signal increases by a factor of N while the incoherent thermal noise grows as \sqrt{N} . Since the electric field emitted by a fully-formed air shower scales linearly with the energy, increasing the SNR of weaker signals lowers the energy threshold of the detector.

Interferometric triggering also reduces the trigger threshold of a radio array by masking out directions with strong sources of anthropogenic backgrounds. First demonstrated in analysis with the TREND experiment [9] we confirm their results at the trigger level using both a single baseline interferometer used to survey multiple sites and a four antenna interferometer at the White Mountain Research Station (WMRS) near Bishop, California. With modest baselines, we were able to reduce the noise-riding trigger thresholds (in power sums) by up to a factor of 2 over a broad field of view. These results can be improved with upgraded antenna beam patterns and longer baselines, both of which are planned for the 2020 season at WMRS. Further details on the site survey and longer term instrumentation study are discussed in these proceedings [11].

The arrival direction of the tau neutrinos can be reconstructed using interferometric techniques as well. The one-sided beamwidth, Θ , of an interferometer constructed from two antennas decreases with increasing bandwidth, Δf , and increasing separation distance between two antennas, L . Coherently summing signals from N antennas each with a voltage signal-to-noise ratio at the antenna SNR_a further narrows the interferometer's beamwidth by a factor of $SNR_a\sqrt{N}$. However, the SNR in the beam, SNR_b also increases by \sqrt{N} . Combining these factors together, the pointing resolution is given by $\delta\theta \sim c/(L\Delta f SNR_b)$. A complete estimate of pointing resolution depends on the layout of the array and will, in general, weight the contributions from different baselines.

3. BEACON Detector Design Studies

By integrating the radio signal over different frequency ranges, we can compare the performance of a high-elevation detector in different frequency bands. We consider two bands in this study: a lower frequency band (30-80 MHz) composed of dipoles with gains of 1.8 dBi and a higher frequency band (200-1200 MHz) composed of horn antennas with gains of 10 dBi. The peak voltage in the time domain V_{peak} from a tau lepton decay received on at the array with gain G_i in a frequency range (f_{lo}, f_{high}) is $V_{peak} = \int_{f_{lo}}^{f_{high}} E_{peak}(f) N \frac{c}{f} \sqrt{\frac{50 \Omega}{377 \Omega} \frac{G_i(f)}{4\pi}} df$.

The signal in both frequency bands is referenced to incoherent thermal noise which is a combination of the system temperature of the amplifier chain used in the detector, $T_{sys} = 140$ K, and the antenna temperature, itself a combination of the galactic noise temperature, $T_{gal}(f)$, and the ground thermal temperature, $T_{ground} = 290$ K, and the ratio, r , of the sky viewed by the antenna (assumed to be 0.5). Because the average galactic noise temperature follows a power law in frequency, the noise temperature assumed in these simulations is dominated by the sky noise for the lower frequency band and by the ground noise temperature in the higher frequency band. Phasing the antennas sums the noise voltage so that $V_{rms} = \int_{f_{lo}}^{f_{high}} \sqrt{Nk[rT_{gal}(f) + (1-r)T_{ground} + T_{sys}]} \sqrt{50 \Omega} df$, which is $14 \mu V$ for the 30-80 MHz band and $10 \mu V$ for the 200-1200 MHz band.

The lower frequency band has a broader radio beam since the region over which the radio emission is coherent is broader at longer wavelengths. However, the peak electric field measured in the higher frequency band is stronger at the Cherenkov angle where the radio signal is coherent. The 30-80 MHz band is appropriate for strong signals originating from higher energy or more distant showers, while the higher frequency band may be better for detecting closer showers or lower energy showers. This is evident in Fig. 3 (left) where the lower frequency band achieves a higher acceptance at energies greater than 3×10^{17} eV, while the higher frequency band has a lower energy threshold. Given the small differences between the two frequency bands, the design

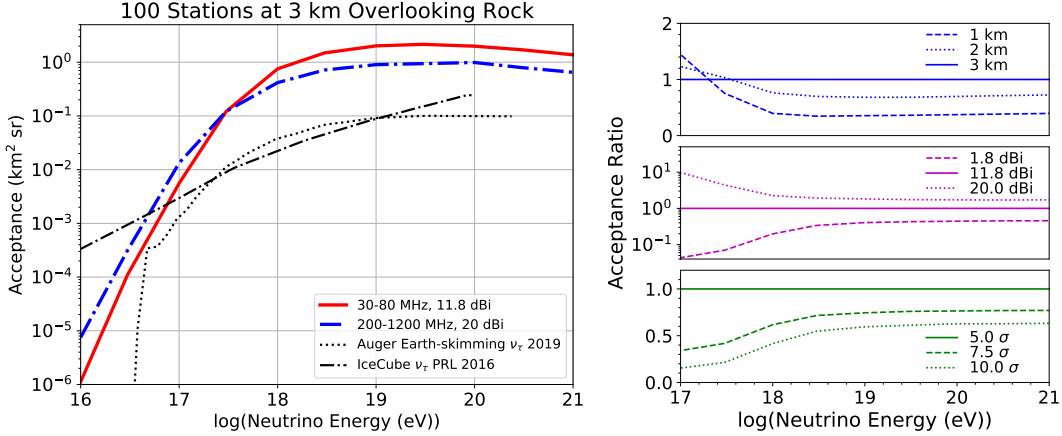


Figure 3: (left) The acceptance of BEACON in two different frequency bands compared with the acceptance of Auger to Earth-skimming tau neutrinos [14] and IceCube to tau neutrinos [15]. Each station comprises 10 antennas with a trigger threshold of 5σ . (right) The ratio of the acceptance of a 30-80 MHz detector for different elevations (top), phased array gains (middle), and trigger thresholds (bottom) relative to the reference design.

frequency band will likely be better determined by the radio-frequency interference local to a given site.

The optimal design of a high elevation radio interferometer depends on several factors shown on the right in Fig. 3 including the detector elevation (top), the effective gain of the phased array (middle), and the average trigger threshold on the beam (bottom).

Detectors at higher elevation view a larger area and are far away enough from the showers that the tau lepton can decay and the air shower can fully develop. This results in a higher acceptance at energies greater than 10^{18} eV as the detectors are placed at higher elevation, but there is a smaller increase in the acceptance going from 1 km to 2 km than from 2 km to 3 km. For lower neutrino energies (10^{17} eV), the BEACON detector is more likely to trigger on events with a shorter distance between the shower and the detector. This suggests that mountain ridges at at least 2 km should be considered for a detector of this design, to maximize both the acceptance at the highest energies and to minimize the number of stations.

The trigger threshold of an impulsive radio receiver is typically implemented as a noise-riding threshold that adjusts to meet a predefined global trigger rate. Fluctuations in the local RFI environment due to anthropogenic backgrounds can cause the thresholds to vary over time and in different beams. A factor of 2 increase in the average threshold from 5σ to 10σ above thermal noise in the beams results in a reduction of the acceptance of 80% at 3×10^{17} eV and 42% at 10^{19} eV. We assume a trigger threshold of 5σ for this study, based on successful implementation of the phased array technique in an ARA station [13].

4. BEACON Array Design

When deciding on array layout, there is a trade-off between digital phasing and angular resolu-

tion along with cosmic-ray rejection. The latter two prefer longer baselines to achieve finer angular resolution, while the phasing technique presumes that the antennas are closely packed enough that each antenna in the array views a similar portion of the shower and is at a similar distance from the showers. At high-elevation mountain geometries, triggered showers are between 10 and 100 km from the detector with lower energy showers triggering at closer distances and therefore steeper angles below the horizon.

This has two important implications. First, the showers are far away enough from the detectors that the signals observed over the core portion of the array are similar. Second, since the higher energy showers especially are expected to be concentrated into angles near the horizon (see Fig. 4 for the range of RF zenith angles observed at a single reference design station), precision angular reconstruction is required for successful background rejection of the more prevalent down-going cosmic rays. A detector observing a 5σ shower at 10 km distance and with 140 m maximum baseline separation between 10 receivers operating in the 30-80 MHz band would have a 0.3° angular resolution. Even in the conservative case that evenly spaces the 10 antennas on a triangular grid, the electric field observed in a beam would be degraded by at most 3%.

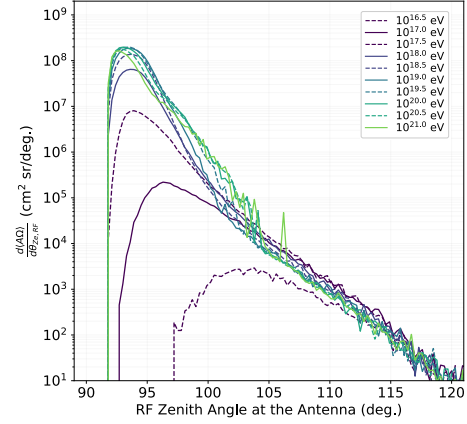


Figure 4: Reference station differential acceptance

5. Discussion

The BEACON reference design can be compared to models predicting an isotropic flux of tau neutrinos, including cosmogenic models (*e.g.* [16, 17]) and extensions to the IceCube flux [4, 3].

Fig. 5 shows the dependence of the expected number of neutrinos for three neutrino models on elevation, frequency band, and the number of antennas included in the phased array assuming a 1:1:1 neutrino flavor ratio. While models that extend to higher energy (Kotera SFR1 [16] and [3]) show a factor of 2 increase in the number of neutrinos going from a 1 km elevation to a 2 km elevation, the gain going from 2 km to 3 km is marginal. Models that cutoff at lower energies [17] or softer power law extensions to the diffuse flux [4] show are insensitive to changes in elevations. Both the lower and higher energy models indicate that the increase in number of neutrinos is linear with phased gain. However, since the number of neutrinos increases linearly with the number of independent stations, we conclude that the preferred station design includes 10 antennas used for both triggering and pointing reconstruction.

The BEACON concept can search for the highest energy tau neutrinos using on phased arrays of radio receivers placed on high-elevation mountains. The concept takes advantage of high individual station acceptance to an isotropic flux while still maintaining sub-degree pointing resolution. We are further pursuing open questions with respect to this design including the point source sensitivity to transient neutrino phenomena, site surveys for different possible BEACON sites, and radio-only triggering on cosmic rays from a high-elevation mountain [11].

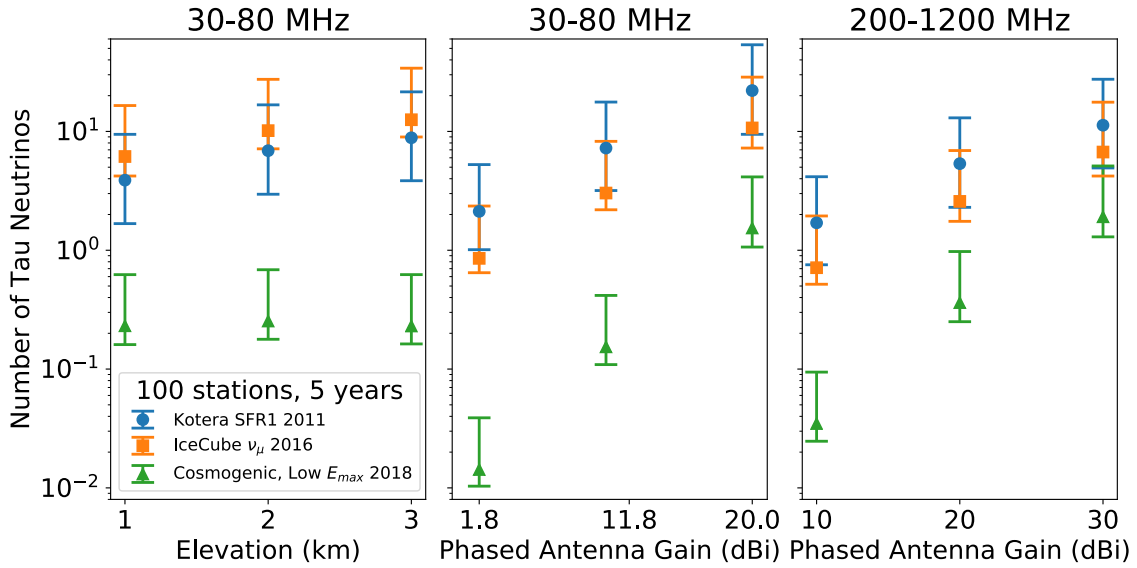


Figure 5: The number of neutrinos expected from models that have high E_{max} [16], extend the IceCube muon flux [3], and predict a lower E_{max} [17] with 100 stations of a BEACON detector with a 30-80 MHz design (left, middle) and a 200-1200 MHz design (right).

References

- [1] M. Ackermann *et al.*, *Bullet. of the AAS* **51** (3), 185 (2019).
- [2] M. Ackermann *et al.*, *Bullet. of the AAS* **51** (3), 215 (2019).
- [3] IceCube, *ApJ* **833**(1), 3 (2016).
- [4] IceCube, *ApJ* **809**(1), 98 (2015).
- [5] IceCube, *Astrophysical Journal* **846**, 136 (2017).
- [6] P. Motloch, N. Hollon, and P. Privitera, *Astroparticle Physics* **54**, 40 (2014).
- [7] J. Alvarez-Muñiz *et al.*, *PRD* **97**(2), 023021 (2018).
- [8] T. Sjöstrand *et al.*, *Computer Phys. Comms.* **191**, 159D177 (2015).
- [9] D. Ardouin *et al.*, *Astropart. Phys.* **34**(9), 717 (2011).
- [10] G. Monroe, Ryan Hallinan *et al.*, *submitted NIM-A* (2019).
- [11] K. Hughes *et al.*, *PoS ICRC* **PS2-104** (2019).
- [12] J. Alvarez-Muñiz *et al.*, *Astroparticle Physics* **35**(6), 325 (2012).
- [13] P. Allison *et al.*, *NIM-A* **930**, 112 (2019).
- [14] Auger, *submitted JCAP*, arXiv:1906.07422v1 (2019).
- [15] IceCube, *PRL* **117**(24), 241101 (2016).
- [16] K. Kotera and A. V. Olinto, *Ann. Rev. of A & A* **49**(1), 119 (2011).
- [17] A. Romero-Wolf and M. Ave, *JCAP* **2018**, 025 (2018).